

identified and recommended during the XXXVII Group Meeting of AICRP-VC held at Tamil Nadu Agricultural University, Coimbatore, Tamil Nadu, in June 2019 for its release in zones I, III and VII based on its performance in the AICRP-VC trials. Finally, cultivar VT 95 was notified as VL Cherry Tomato 1 during the meeting of the Central Subcommittee on Crop Standard Notification and Release for Horticultural Crops² and it was held in virtual mode on 28 October 2020.

The plants of VL Cherry Tomato 1 are semi-indeterminate type, 115–130 cm in height, with thin stem having 2–4 primary branches, yellow flowers with non-exserted style position, and 90–120 fruits per plant. Fruits are small in size (15–25 g), oval with a smooth surface, 10–20 fruits per cluster, two locules per fruit, and they are attractive red colour with 2.8–3.0 mm thick flesh (Figure 1). The plant matures early (60–75 days for first picking after transplanting) and 50% flowering takes place 30–40 days after transplanting. Fruits possess high lycopene (7.19 mg/100 g) and high vitamin C (75.62 mg/100 g) contents (Table 4). The suitable transplanting time for its cultivation in the mid-hills conditions (1000–1500 m amsl) of India is the first week of March and April–July under

open field and poly-house (naturally ventilated) conditions respectively.

Seeds of VL Cherry Tomato 1 are being multiplied every year and are available to Indian scientists and farmers upon request at the ICAR-VPKAS. The seeds of this variety have also been deposited at ICAR-NBPGR under accession no. IC 584764. Seed requests from outside India may be addressed to the Director, ICAR-NBPGR.

1. Hedau, N. K., Dhar, S., Mahajan, V., Agarwal, P. K. and Bhatt, J. C., *Hortscience*, 2014, **49**(1), 105–106.
2. GoI, *The Gazette of India*, Notification No. SO 1480 (E), 3-73/2020-SD. IV, Controller of Publications, New Delhi, 1 April 2021.

ACKNOWLEDGEMENTS. We thank the Director, ICAR-Vivekananda Parvatiya Krishi Anusandhan Sansthan (VPKAS) for providing guidance and support during this study, and Shankar Lal, O. P. Vidyarthi and Manoj Bhatt (VPKAS) for technical assistance. We also thank ICAR-NBPGR, New Delhi and AVRDC, Taiwan for providing the germplasm line (CH 154), and the Indian Council of Agricultural Research, New Delhi for providing the necessary facilities and funds to carry out this study.

Received 15 February 2022; accepted 11 April 2022

N. K. HEDAU^{1,*}
SHRI DHAR²
G. V. CHAUDHARI³
P. K. AGARWAL⁴
JAGDISH C. BHATT¹
M. TUTI⁵
K. S. HOODA⁶
K. K. MISHRA¹
R. S. PAL¹

¹ICAR-Vivekananda Parvatiya Krishi Anusandhan Sansthan, Almora 263 601, India

²ICAR-Indian Agricultural Research Institute, New Delhi 110 012, India

³ICAR-Central Coastal Agricultural Research Institute, Ela, Old Goa 403 402, India

⁴Odisha University of Agriculture and Technology, Bhubaneswar 751 003, India

⁵ICAR-Indian Institute of Rice Research, Hyderabad 500 030, India

⁶ICAR-National Bureau of Plant Genetic Resources, PUSA Campus, New Delhi 110 012, India

*For correspondence.
e-mail: Nirmal.Hedau@icar.gov.in

Sub-alpine Himalayan birch in cold arid Lahaul-Spiti, Himachal Pradesh, India: a proxy of winter/early spring minimum temperature

The recent warming of the earth and its imminent consequences in the form of accelerated climatic variability threatening humankind is the biggest global concern. The IPCC-AR6 report revealed that the global surface temperature had increased faster since 1970 compared to any other 50-year period in the last 2000 years¹. Recently, the Conference of the Parties (COP26), held in Glasgow from October–November 2021, highlighted the global impact of climate change. The COP countries reaffirmed the Paris Agreement goal of limiting the increase in the global average temperature to well below 2°C above pre-industrial levels and pursuing efforts to limit it to 1.5°C and limit the emission of greenhouse gases to net zero in the future. However, the role of human-induced changes on natural variability in climate is not yet well understood. Human-induced

changes have a marked impact on climate change^{2–4}, and centred manifold in densely populated urban areas relative to the high-altitude regions. Difficult orographic terrains in the Himalayan regions restrict the anthropogenic encroachments and near pristine environments are met in high elevation areas. Observational records from the Himalayan regions and Tibetan Plateau show warming in the minimum/winter temperature^{5,6}, posing serious concerns for the high-altitude ecology, glaciers and rivers originating from the glaciated regions. Recently, in February 2021, a flash flood due to glacier breakdown occurred in Chamoli, Uttarakhand, India, causing huge socio-economic losses^{7,8}. Glacier breakdown during the winter season over the high-altitude Himalayan region could be due to increased minimum/winter temperature and/or increased snow load. Such climatic

challenges are crucial for the Himalayan region in terms of ecology, life and sustainable development. However, our understanding of climate variability is limited largely due to the short observational records. Trees growing in the remote high-altitude Himalayan regions have the potential to reveal climate variability in the long-term perspective through annually resolved growth-ring sequences. Therefore, in the present study, we analysed the growth of the high-elevation Himalayan birch (*Betula utilis*) with minimum temperature from Western Himalaya, India.

Himalayan birch, a prominent broadleaf tree, grows mostly in harsh, frigid climatic conditions in the Himalayas. The tree has the unique ability to survive in cold alpine regions and its growth-ring patterns precisely document the ambient environmental changes. The Himalayan birch trees are

Table 1. Detailed statistics of Himalayan birch tree-ring chronologies developed from Yoche Valley, Himachal Pradesh, India. The chronology statistics was evaluated for $EPS \geq 0.85$, AD 1752–2014

Site	Latitude (N)	Longitude (E)	Core/tree	Chronology span	Chronology with $EPS \geq 0.85$	MI	MS	SD	AR1
Yoche	32°37'13.0"	77°15'56"	34/21	AD 1652–2014 (363 yrs)	1752–2014	1.00	0.265	0.270	0.32
Darcha	32°38'26.0"	77°13'35.3"	27/25	AD 1689–2016 (328 yrs)	1749–2016	1.00	0.268	0.279	0.37

EPS, Expressed population signal; MI, Mean index; MS, Mean sensitivity; SD, Standard deviation; AR1, First autocorrelation.

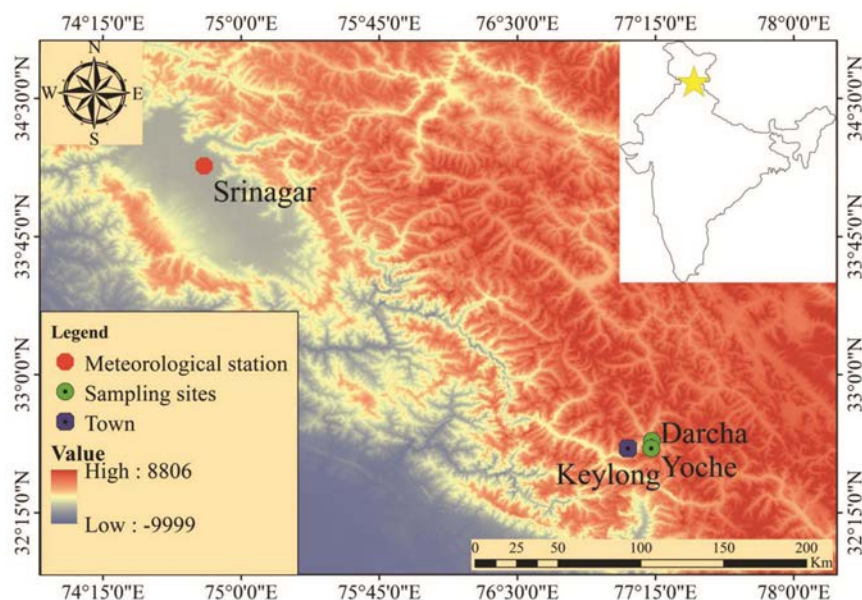


Figure 1. Location map of tree-ring sampling sites and meteorological stations used in the present study. Location of the sampling region is marked by a yellow-coloured star.

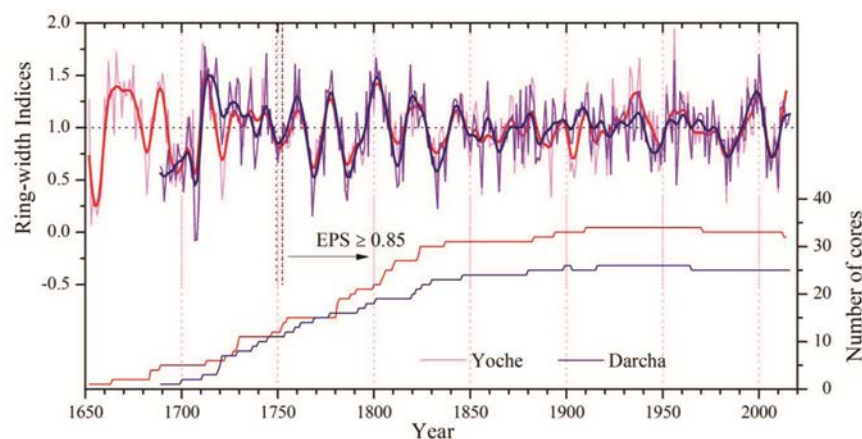


Figure 2. Himalayan birch tree-ring-width chronologies from Lahaul-Spiti, Himachal Pradesh, India, along with the number of samples.

mostly found at high-elevation sites in the Western Himalayas, which are completely snow-covered during winter. In the present study Himalayan birch forests at an elevation ranging from 3500 to 3800 m amsl were surveyed over the cold arid Lahaul-Spiti, Himachal Pradesh, India. The Yoche and Darcha sites were identified where

Himalayan birch trees grow in isolated patches (Figure 1). Tree-ring increment cores from both the sites were collected during two field trips in 2014 and 2016, using increment borer at breast height. Utmost care was taken during the collection of samples as the trees were damaged in the valley due to the snowfall. Trees

without any apparent physical injury were selected for sampling and two cores were generally collected from a tree. However, due to steep slopes only one core from a tree was extracted from the Darcha site. A total of 46 healthy trees were identified and 61 increment cores were taken from both sites (Table 1). The extracted samples were brought to the laboratory and air-dried at room temperature. The samples were then mounted in wooden frames facing cross-surface upward and polished with different grades of abrasive until the growth rings became visible under a stereo zoom binocular microscope. The polished samples were used in cross-dating to assign the exact calendar year to growth rings. The skeleton plotting method was used to cross-date the tree-ring samples⁹. The ring widths of precisely cross-dated samples were measured with a resolution of 0.01 mm using the LINTAB (Rinntech, Germany) measuring machine attached to a personal computer¹⁰. The COFECHA program was used to test the dating quality of the samples¹¹. The samples/sample portions observed with errors in COFECHA analysis were remeasured and dating errors resolved. The tree growth over a region is influenced by various internal (genetic constitution, biological age) and external (competition among trees for nutrients, sunlight and diseases) factors and climate. The non-climatic factors which influence tree growth were minimized and removed while common climate signals were strengthened using standard procedures¹².

To standardize the ring-width measurement series, the signal-free method was used in the present study¹³. The RCSsig-Free_v45 program (available at the Tree-Ring Laboratory, Lamont Doherty Earth Observatory, Columbia; <http://www.ldeo.columbia.edu/tree-ring-laboratory/resources/software>) was used to standardize the ring-width measurement series. The measurement series were detrended using cubic smoothing spline, which preserved 50% of the amplitude over a wavelength of two-thirds of the series length¹⁴. To stabilize the variance, data-adaptive power transformation was used before detrending¹⁵. By calculating

biweight robust mean, individual ring-width measurement series were combined with mean chronology¹⁶ (Figure 2). The expressed population signal (EPS) threshold of ≥ 0.85 , which decreases back in time with the decreasing number of samples, was used to select chronology length for the climatic studies¹⁷. Table 1 gives the chronology statistics, including chronology length, samples used, mean sensitivity, standard deviation and EPS threshold exceeding 0.85.

The oldest Himalayan birch tree age observed in the present study was 363 years (AD 1652–2014) from Yoche and 328 years (AD 1689–2016) from Darcha sampling sites. Both site chronologies showed significantly strong Pearson correlation ($r = 0.835$, 1752–2014, $P < 0.0001$). To analyse the climate and tree growth relationship, we performed a response function analysis using the climate data of Srinagar meteorological station situated ~ 165 km from the sampling sites. This is the only station having minimum and maximum temperature records from 1995 to 2019 close to the study region. The instrumental records of Srinagar revealed that the minimum temperature goes below zero in December (-1.9°C) and January (-1.3°C). The precipitation records revealed that two-thirds of the annual precipitation occurred in the winter and spring seasons due to the mid-latitude westerlies. However, the summer monsoon precipitation has less influence over the cold-arid Lahaul-Spiti as the Pir Panjal peaks act as an orographic barrier. To understand the relationship between tree growth and climate, we used the first principal component (PC#1) having eigenvalue > 1 . PC#1 showed 91.7% of the common variance of the chronologies and revealed the common climate forcing controlling the growth of trees at both sampling sites. The response function analysis was performed using DENDROCLIM2002 (ref. 18). The PC#1 relationship with monthly temperature (minimum, maximum and mean) and precipitation for the period 1996–2014 were explored. The climate and tree growth relationship showed a relatively weak correlation with maximum and mean temperature. Although PC#1 revealed a significant correlation with maximum temperature for October and November in the previous year and February, March, June and July in the current year (figure not shown), the strongest correlation was observed with minimum temperature for February and March of the current year. The minimum temperature showed a con-

tinuous negative correlation in the winter and early spring from December to March and a positive correlation in summer from April to July (Figure 3). A strong and significant negative correlation was noted in February and March, and significant positive relationship in July with minimum temperature. The response function analysis did not show any significant correlation with precipitation during any month.

We also calculated Pearson correlation of PC#1 with seasonized February–March minimum and maximum temperature and noted a strong correlation with minimum temperature (-0.78 , 1995–2014, $P < 0.0001$) in comparison to maximum temperature (-0.60 , 1995–2014, $P = 0.005$). The strong

correlation of PC#1 with minimum temperature revealed that winter and early spring minimum temperature significantly contribute to the radial growth advancement of trees over the sub-alpine region of the Himalayas. Further, the response function analysis revealed that the minimum temperature in winter inversely affects tree growth, while tree growth is directly affected during summer.

The relationship of tree-ring chronology with winter minimum temperature was stronger compared to the summer season, which indicates that the Himalayan birch is sensitive to winter temperature. During winter, heavy precipitation occurs in the high-altitude Western Himalayas and snow

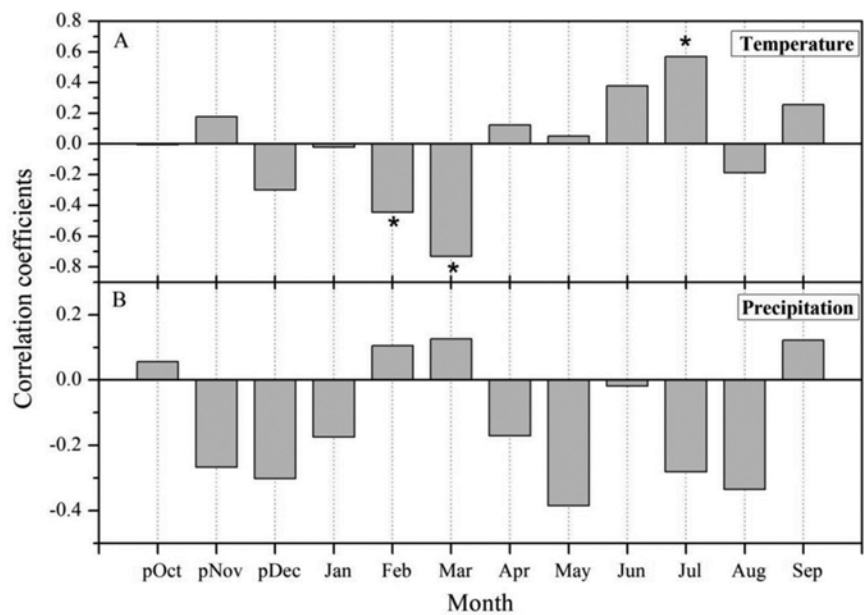


Figure 3. Response function analysis of PC#1 with minimum temperature and precipitation. Asterisk represents correlations significant at the 95% confidence level.

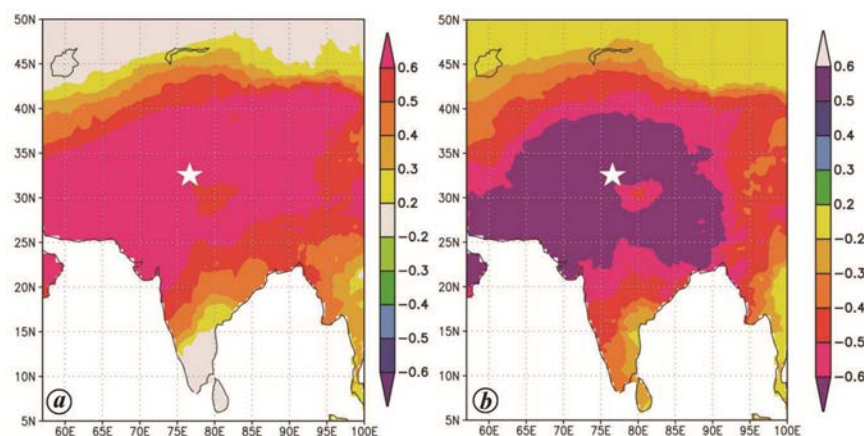


Figure 4. The cross-field spatial correlation of (a) observational minimum temperature and (b) PC#1 with gridded minimum temperature. Star represents the tree-ring sampling location.

covers the region for a longer period. As the temperature decreases due to snowfall during winter, a thick blanket of snow cover insulates the root system from the low atmospheric temperature. The thick snow cover protects the vegetation from dry and icy atmospheric conditions while also maintaining moisture supply^{19,20}. On the contrary, higher water stress in plants and desiccation in seedlings exposed directly to sunlight over snow-free land surfaces during winter were reported in the sub-alpine zones²¹. Hence, it can be concluded that the thick snow cover during severe cold winters in the sub-alpine zones breaks the tree-root connection with the cold atmospheric conditions and supports tree growth in early spring as the snow starts melting.

To further validate the relationship of the Himalayan birch with winter minimum temperature over the high-altitude Lahaul-Spiti region, we performed the cross-field correlation of the observed minimum winter temperature and PC#1 with gridded minimum temperature available at KNMI Climate Explorer. The spatial correlation of instrumental temperature data and PC#1 was analysed for February–March of the current year during 1995–2019, for which the records were available. The spatial correlation analyses revealed a negative correlation of PC#1 with gridded minimum temperature, similar to that noted with the observed winter minimum temperature (Figure 4). Such a strong correlation reveals the reliability of tree-ring chronologies of Himalayan birch to understand the role of minimum winter temperature on tree radial growth advancements. The strong relationship between high-altitude Himalayan birch trees and minimum temperature has

been explored in the present study. This study further reveals that Himalayan birch chronologies can be used to develop long-term minimum temperature reconstructions.

1. IPCC. In *Climate Change 2021: The Physical Science Basis. Contribution of Working Group I to the Sixth Assessment Report of the Intergovernmental Panel on Climate Change* (eds Masson-Delmotte, V. et al.), Cambridge University Press, 2021.
2. Bollasina, M. A., Ming, Y. and Ramaswamy, V., *Science*, 2011, **334**(6055), 502–505.
3. Mgbemene, C. A., Nnaji, C. C. and Nwozor, C., *Environ. Sci. Technol.*, 2016, **9**(4), 301–316.
4. Lelieveld, J., Klingmüller, K., Pozzer, A., Burnett, R. T., Haines, A. and Ramathan, V., *Proc. Natl. Acad. Sci. USA*, 2019, **116**(15), 7192–7197.
5. Liu, X., Yin, Z. Y., Shao, X. and Qin, N., *J. Geophys. Res.: Atmos.*, 2006, **111**(D19), 1–19.
6. Ren, Y. Y. et al., *Adv. Climate Change Res.*, 2017, **8**(3), 148–156.
7. Shugar, D. H. et al., *Science*, 2021, **373**(6552), 300–306.
8. Pandey, V. K. et al., *Geomat. Nat. Hazards Risk*, 2022, **13**(1), 289–309.
9. Stokes, M. A. and Smiley, T. L., *An Introduction to Tree-Ring Dating*, University of Chicago Press, Chicago, USA, 1968.
10. Rinn, F., TSAP-Win time series analysis and presentation for dendrochronology and related applications, version 0.53 for Microsoft Windows, Rinn Tech, Heidelberg, Germany, 1996, p. 110.
11. Holmes, R. L., *Tree-Ring Bull.*, 1983, **43**, 69–78.
12. Fritts, H. C., *Tree-Rings and Climate*, Academic Press, London, UK, 1976, p. 567.
13. Melvin, T. M. and Briffa, K. R., *Dendrochronologia*, 2008, **26**, 71–86.
14. Cook, E. R. and Peters, K., *Tree-Ring Bull.*, 1981, **41**, 45–53.
15. Cook, E. R. and Peters, K., *Holocene*, 1997, **7**, 361–370.
16. Cook, E. R., Ph.D. thesis, University of Arizona, Tucson, Arizona, USA, 1985, p. 171.
17. Wigley, T. M. L., Briffa, K. R. and Jones, P. D., *J. Climate Appl. Meteorol.*, 1984, **23**, 201–213.
18. Biondi, F. and Waikul, K., *Comput. Geosci.*, 2004, **30**, 303–311.
19. Ide, R. and Oguma, H., *Ecol. Inform.*, 2013, **16**, 25–34.
20. Desai, A. R. et al., *Environ. Res. Lett.*, 2016, **11**(2), 024013.
21. Frey, W., *Arct. Antarct. Alp. Res.*, 1983, **15**(2), 241–251.

ACKNOWLEDGEMENTS. V.S., K.G.M. and A.K.Y. thank Dr Vandana Prasad (Director, Birbal Sahni Institute of Palaeosciences, Lucknow) for providing the necessary facilities for this study. We also thank the Forest Department, Himachal Pradesh for logistic support during field work and India Meteorological Department for providing meteorological data.

Received 9 February 2022; revised accepted 23 May 2022

VIKRAM SINGH^{1,*}
KRISHNA G. MISRA^{1,*}
AKHILESH K. YADAVA¹
RAM R. YADAV²

¹Birbal Sahni Institute of Palaeosciences,
53, University Road,
Lucknow 226 007, India

²Wadia Institute of Himalayan Geology,
33, G.M.S. Road, Vijay Park,
Dehradun 248 001, India

*For correspondence.
e-mail: vnegi850@gmail.com;
kgmisrabsip@gmail.com